

Neurocognitive Pathways in Attention-Deficit/Hyperactivity Disorder and White Matter Microstructure

Supplementary Information

Supplemental Methods and Materials

Case-Control Matching

This study was part of a larger NIMH-funded study on the neurobiology of ADHD, which collected a total of 185 individuals with DTI scans who met the diagnostic inclusion and exclusion criteria, as described in the primary manuscript. Four additional individuals were excluded for less than two complete cognitive tasks ($n = 3$), or lack of effort on all cognitive tasks ($n = 1$). Several individuals were removed from the current analysis for DTI quality issues, including rare magnetic leakage artifacts ($n = 1$), improper FOV placement ($n = 2$), and less than three DTI scan runs ($n = 3$). One individual was also removed for DTI movement issues, such that this individual showed greater than 3 mm of movement in any direction across more than one DTI scan run, leaving the overall concatenated image of poor quality. Of the final 174 individuals available, 67 were diagnosed with ADHD combined subtype. These individuals were carefully case-control matched with 68 non-ADHD youth who had at least two cognitive tasks and complete quality DTI scans.

Missingness

A total of 38 individuals (28% of the sample) included in the subsequent analyses had at least one missing neurocognitive task. No one task was missing more than 13% of the sample. Little's MCAR test suggested that this data were missing at random, $\chi^2_{104} = 115.41$, $p = .21$.

Missingness was not related to diagnostic group, $\phi = -0.13$, $p = .14$. Regressions were then performed to impute missing values from the larger set of variables collected from the six tasks, including the primary dependent variables included in subsequent analysis, as well as age, IQ and gender.

Normalization

Prior to confirmatory factor analysis and principal component analysis, the SKIP RT was natural log transformed and all variables z-transformed and reoriented so that positive component loadings indicated relatively greater performance or ability. Thus, all variables entered into confirmatory factor analysis and principal component analysis were z-scored, with means of 0 and standard deviations of +/- 1. Both skew and kurtosis were within acceptable ranges for normality assumptions (skew < |0.7|, kurtosis < |1.5|). See Supplementary Table S1 for descriptive statistics.

Individual component scores from the three principal components identified by principal component analysis were also examined for normality assumptions. Both skew and kurtosis were within acceptable ranges for normality assumptions (skew < |0.5|, kurtosis < |0.4|). See Supplemental Table S2 for descriptive statistics.

DTI Movement and Quality Checking

For quality checking purposes, each participant's DTI timeseries was visually inspected, and 6 participants were removed for issues that could result in poorer signal-to-noise ratios (as discussed above). In addition to standard realignment, B₀ inhomogeneity and eddy current correction, any participant with movement greater than 3 mm in any x, y, or z direction across

more than one of three DTI scans was removed ($n = 1$), and any scan-to-scan movement greater than 2 mm was removed prior to tensor calculation. This 2 mm threshold was selected based upon inspection of outliers across all scan-to-scan displacement values across the whole sample. Finally, to ensure only valid non-movement-contaminated images were used for robust and accurate tensor calculation, participants were included in analyses if more than 90% of original slices/directions of DTI scans were of quality and intact, and no more than 1/3 of the same slice DTI direction was removed.

Supplemental Results

Group level t -tests of ADHD and non-ADHD youth, while covarying for nuisance variables (age, gender and IQ) found no FA differences in whole-brain analyses using TFCE *corrected* $p < .05$ significance thresholds. When this significance threshold was reduced to uncorrected $p < .01$ without TFCE, small regions of significant differences between ADHD and non-ADHD youth emerged. ADHD youth showed lower FA in numerous regions, including brainstem, subcortical, parietal and frontal areas. ADHD youth also evidenced greater FA in several regions, particularly cerebellum, occipital, and various frontal areas. Notably, while these regions overlap with findings from previous work, these sparse tract-based findings do not survive rigorous corrections for multiple comparisons. See Supplemental Figure S2 for full presentation of these results.

Supplementary Table S1. Normalization and transformation outcomes of primary neuropsychological performance measures for ADHD and non-ADHD adolescents.

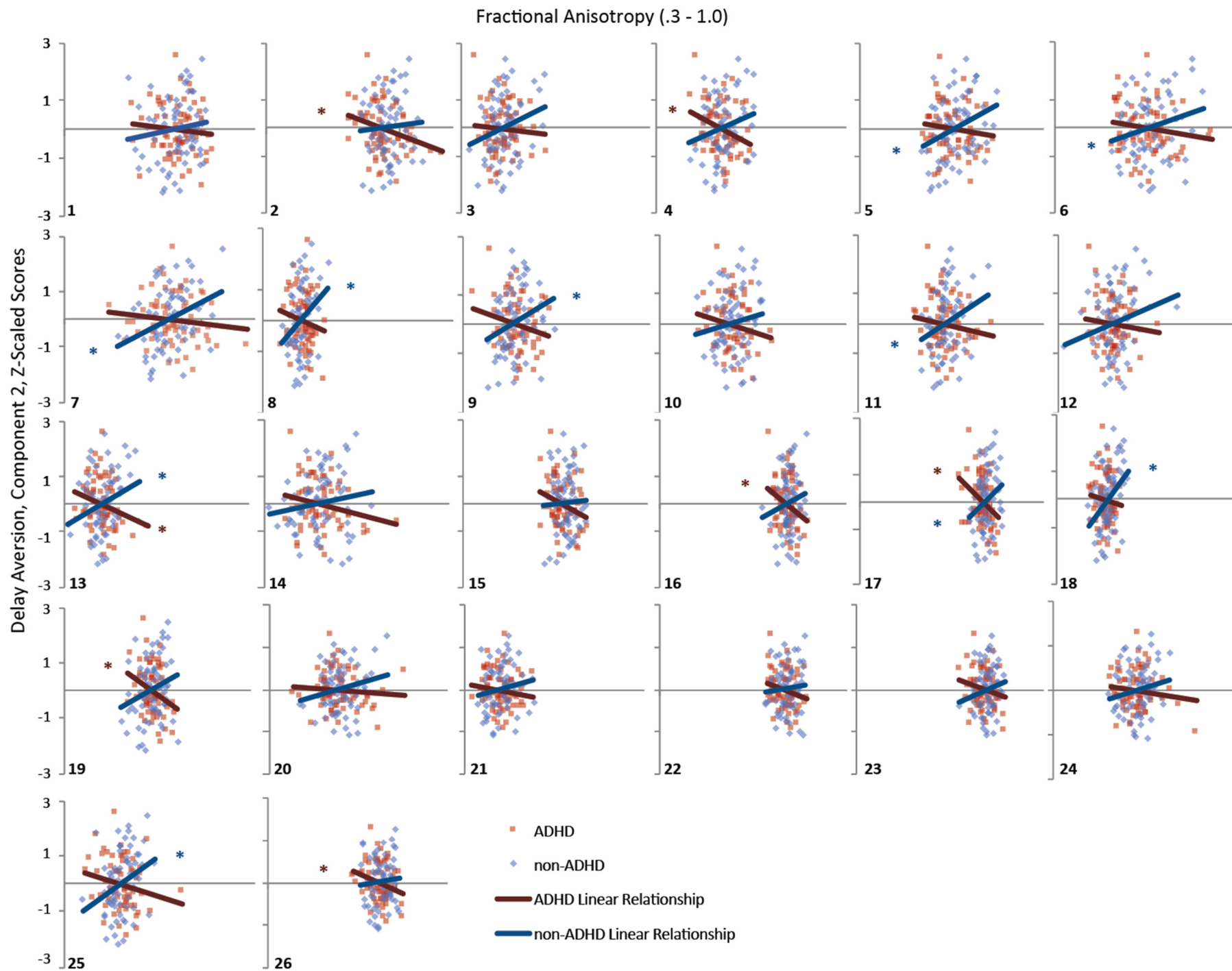
Neuropsychological Performance	Skewness (SE)	Kurtosis (SE)
Conner's CPT-II, Commissions Errors	0.53 (0.21)	-0.10 (0.41)
Stop Signal Reaction Time	0.12 (0.21)	1.39 (0.41)
Delayed Memory Test, Commission Error %	0.27 (0.21)	-0.20 (0.41)
Single Key Impulsivity Paradigm, Average IRT	0.36 (0.21)	-0.76 (0.41)
Experiential Delay Task	-0.44 (0.21)	-0.41 (0.41)
Delay Discounting Questionnaire	0.69 (0.21)	-0.62 (0.41)

Note. All normalized, transformed neuropsychological performance measures had a mean of 0.00 and standard deviation of 1.00.

Supplementary Table S2. Descriptive statistics for each principal component identified from PCA.

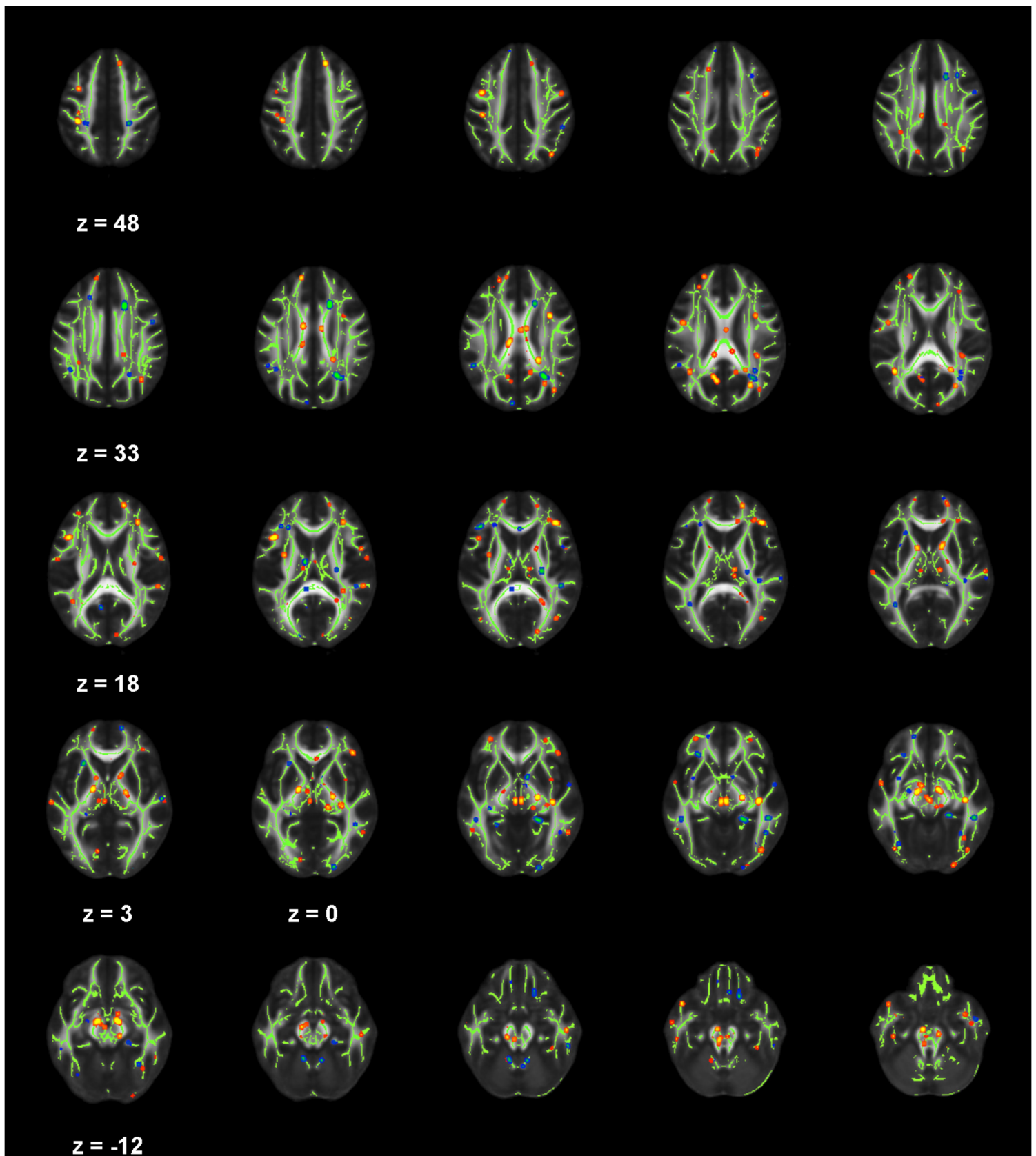
Component	Skewness (SE)	Kurtosis (SE)
Disinhibition	0.48 (0.21)	0.32 (0.41)
Delay Aversion	0.19 (0.21)	-0.35 (0.41)
Impulsive Choice	0.48 (0.21)	-0.25 (0.41)

Note. All principal components had a mean of 0.00 and standard deviation of 1.00.



Supplemental Figure S1. Scatterplots of each region of interest and relationship between fractional anisotropy and Delay Aversion (Component 2) scores for ADHD and non-ADHD separately. Lines represent linear associations for each group. X-axis depicts fractional anisotropy (FA) from 0.3 to 1.0 on all graphs; Y-axis depicts Delay Aversion Component 2 scores. Asterisks represent significant Pearson correlations for the indicated region of interest (ROI) in the corresponding group (red = ADHD, blue = non-ADHD), as reported in Table 3 in the primary manuscript. Number in bold at the bottom of each graph corresponds to each ROI, listed below, in the same order as described in Table 3 in the primary manuscript.

#	Scatterplot ROI Label
	FRONTAL
1.	Body of Corpus Callosum
2.	Genu of Corpus Callosum (Forceps Minor)
3.	Left Anterior Corona Radiata
4.	Right Anterior Corona Radiata
5.	Right Anterior Corona Radiata (Forceps Minor)
6.	Right Tapetum
	OCCIPITAL
7.	Splenium of Corpus Callosum (Forceps Major)
	TEMPORAL
8.	Left Inferior Longitudinal Fasciculus
9.	Left Uncinate Fasciculus/Inferior Fronto-Occipital Fasciculus
10.	Right Superior Longitudinal Fasciculus
	PARIETAL
11.	Left Posterior Corona Radiata (Corticospinal Tract)
12.	Right Posterior Corona Radiata
13.	Left Superior Corona Radiata
	SUBCORTICAL
14.	Left Anterior Limb of Internal Capsule (Ant Thalamic Radiation)
15.	Right Anterior Limb of Internal Capsule (Ant Thalamic Radiation)
16.	Left Posterior Limb of Internal Capsule (Corticospinal Tract)
17.	Right Posterior Limb of Internal Capsule (Corticospinal Tract)
18.	Left Retrolenticular Part of Internal Capsule
19.	Right Retrolenticular Part of Internal Capsule
20.	Right Posterior Thalamic Radiation
21.	Left External Capsule
	BRAINSTEM
22.	Left Cerebral Peduncle (Corticospinal Tract)
23.	Right Cerebral Peduncle (Corticospinal Tract)
24.	Left Superior Cerebellar Peduncle
25.	Left Corticospinal Tract
26.	Left Medial Lemniscus



Supplemental Figure S2. White matter regions from tract-based spatial statistics (TBSS) analysis *t*-tests where fractional anisotropy was significantly different between ADHD compared to non-ADHD adolescents at uncorrected $p < .01$ thresholds. Red-yellow indicates regions where FA in ADHD youth is less than non-ADHD youth, whereas blue-green indicates regions where FA in ADHD youth is greater than non-ADHD youth.